DOI 10.1007/s10946-021-09987-w
Journal of Russian Laser Research, Volume 42, Number 4, July, 2021

A TUNABLE SINGLE- AND TRIPLE-WAVELENGTH Nd:GGG LASER IN THE 1.3 μm RANGE WITH 880 nm LD DIRECT PUMPING

Muhan Wang, Haifeng Lin,* Ruizhen Mu, Wenzhang Zhu, and Feibing Xiong

Fujian Provincial Key Laboratory of Optoelectronic Technology and Devices
Xiamen University of Technology
Xiamen 361024, China

School of Optoelectronic and Communication Engineering
Xiamen University of Technology
Xiamen 361024, China

*Corresponding author e-mail: hflin@xmut.edu.cn

Abstract

We report a single- and triple-wavelength Nd:GGG laser operating in the 1.3 μm wavelength range with 880 nm laser diode pumping directly into the $^4F_{3/2}$ emitting level. For a pump power of 24.85 W, a single wavelength of 1331 nm is obtained with an output power of 2.95 W and a slope efficiency of 15.9%. By inserting a 0.1 mm thick BK7 glass etalon and adjusting its tilting angle, we achieve tunable lasing wavelengths of 1323, 1331, 1336, 1338, and 1346 nm with maximum output powers of 1.94, 2.46, 1.92, 1.80, and 1.17 W, as well as slope efficiencies of 8.07%, 10.25%, 7.98%, 7.48%, and 4.85%, respectively. We realize simultaneous triple-wavelength laser at 1323, 1331, and 1336 nm, for the first time, up to our knowledge, with a maximum output power of 1.66 W and a slope efficiency of 6.6%.

Keywords: Nd:GGG crystal, single- and triple-wavelength laser, LD direct pumping.

1. Introduction

1.3 μm lasers have wide applications in optical fiber communications, optical sensor positioning, laser medicine, biological imaging, precision micromachining, etc. [1, 2]. In addition, 1.3 μm multiwavelength lasers are useful for the newly developed terahertz wave generation based on nonlinear optical difference-frequency method [3]. It is a common knowledge that 1.3 μm wavelength laser can be obtained on the $^4F_{3/2}$—$^4I_{13/2}$ transition in Nd^{3+}; there are examples such as Nd:YAP, Nd:GGG, Nd:$YAlO_3$, Nd:$GdVO_4$, Nd:LuAG, Nd:YAG, Nd:$LuVO_4$, Nd:GYSGG lasers, etc. [4–15]. Compared with other Nd^{3+}-doped crystals, the Nd:GGG crystal has good mechanical properties, excellent thermal performance, large fluorescence lifetime [16], and wide absorption wavelength band, which reduces the sensitivity dependence on the diode laser wavelength [17]. The concentration of Nd^{3+} in GGG can reach 4% or even be higher [18, 19]. Therefore, a laser with low threshold and high light conversion efficiency can be more easily realized in the Nd:GGG crystal [20, 21].

808 nm LDs are usually used as the pump source of all-solid-state Nd^{3+}-doped lasers, due to the relatively-high absorption efficiency of Nd^{3+} for 808 nm wavelength light. However, for 808 nm LD pumping, the resulting nonradiative transition increases the thermal effect of the crystal, which limits

Manuscript submitted by the authors in English on April 13, 2021.

 1071-2836/21/4204-0494

increase in the laser output power and reduces the laser beam quality. The 880 nm LD pumping is an effective means to reduce the thermal effect [22], because there is no thermal relaxation during the stimulated radiation process. At the same time, due to the fact that Nd^{3+} substituting Gd^{3+} has only weak concentration quenching, the low absorption factors of Nd^{3+} for 880 nm can be overcome by increasing the doping concentration of Nd^{3+}. In this paper, we achieve a 1331 nm Nd:GGG laser with an output power of 2.95 W and a slope efficiency of 15.9% by 880 nm LD pumping of 24.85 W. At the same time, by inserting 0.1 mm thick BK7 glass etalon in order to select the oscillation wavelength, we achieve 1323, 1331, 1336, 1338, and 1346 nm single wavelength lasers and obtain the simultaneous triple-wavelength output at 1323, 1331, and 1336 nm. For the best of our knowledge, this is the first time when the triple-wavelength Nd:GGG laser pumped by 880 nm LD is realized.

2. Experimental Setup

A schematic of the experimental setup is shown in Fig. 1. A simple plane-concave resonator with a length of 50 mm is employed. The pump source is a commercially available fiber-coupled laser diode (QPC Inc.), which delivers a maximum output power of about 50 W at the center wavelength equal to 880 nm. The core diameter of the coupling fiber and the numerical aperture are 400 μm and 0.22, respectively. The coupling lens and focusing lens are both achromatic doublets with focal lengths of 50 mm. The input mirror (IM) is a flat mirror, which has a maximum transmission (> 90%) at 880 nm and high reflectivity (> 99.9%) at 1.33 μm. In addition, IM has broad transmission of about 90% at 1.06 μm to suppress those potential high-gain lasing wavelengths. The output coupler (OC) is a concave mirror with the radius of curvature equal to 100 mm and a transmission of 4.0% for 1.33 μm.

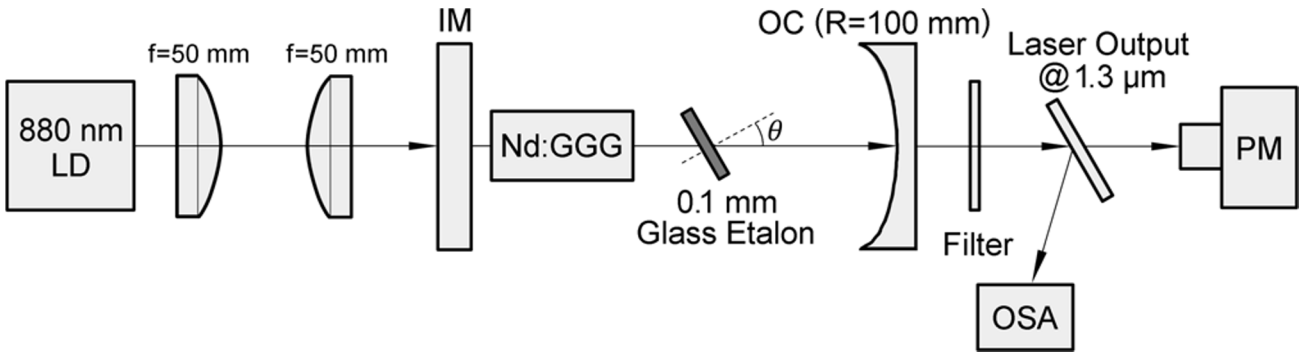

Fig. 1. Schematic of 880 nm diode-pumped Nd:GGG lasers.

The Nd:GGG crystal used in the experiments has a Nd^{3+} concentration of 0.8 at.% and dimensions of 3×3×8 mm. To reduce the thermal load accumulated under high power pumping, the laser crystal is wrapped with an indium foil and mounted in a copper holder connected to the cooling water with an initial temperature of 18±0.1°. During wavelength selection, a BK7 glass etalon is used to modulate the intracavity losses with respect to those potential lasing wavelengths. The laser spectrum is measured by an optical spectrum analyzer (OSA, AQ6370, Yokogawa) with a spectral resolution of 0.1 nm, and the average output power is measured by a laser power meter (919P-050-26, Newport).

3. Results and Discussions

In Fig. 2, we show the fluorescence emission spectrum in the range of 1.3 μm of Nd:GGG crystal pumped by an 880 nm LD. One can see five lasing wavelengths of 1323, 1331, 1336, 1338, and 1346 nm. According to [23], these emission lines are assigned to Nd^{3+} emission transitions occurring between the two Stark components R_1 and R_2 of the $^4F_{3/2}$ emitting multiplet and the five Stark sublevels X_1, X_2, X_3, X_4, and X_5 of the lower-lying $^4I_{13/2}$. Moreover, according to [24], the above five emission lines occur with emission cross sections of about $3.15 \cdot 10^{-20}$, $3.9 \cdot 10^{-20}$, $3.5 \cdot 10^{-20}$, $2.0 \cdot 10^{-20}$, and $2.15 \cdot 10^{-20}$ cm^2, respectively. Therefore, without intracavity frequency selection (i.e., BK7 etalon is not inserted), and due to its largest emission cross section, lasing action will occur at about 1331 nm. The output spectrum with a center wavelength of 1331.2 nm is sketched in Fig. 3, and only accompanied by a very weak laser emission at about 1336 nm. The dependence of the output power on the incident pump power at 880 nm LD is shown in Fig. 3. When the incident pump power is 24.85 W, the maximum output power is found to be up to 2.95 W, and the threshold power is about 1.13 W; the corresponding slope and optical conversion efficiency are 15.9% and 11.9%, respectively.

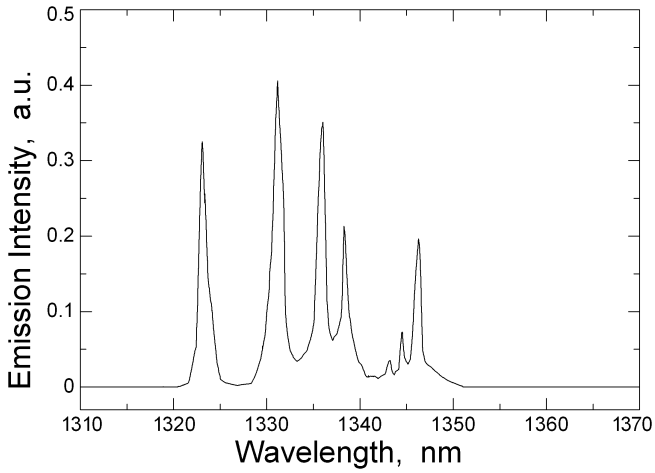

Fig. 2. Fluorescence spectrum of a Nd:GGG crystal in the range of 1310 to 1370 nm.

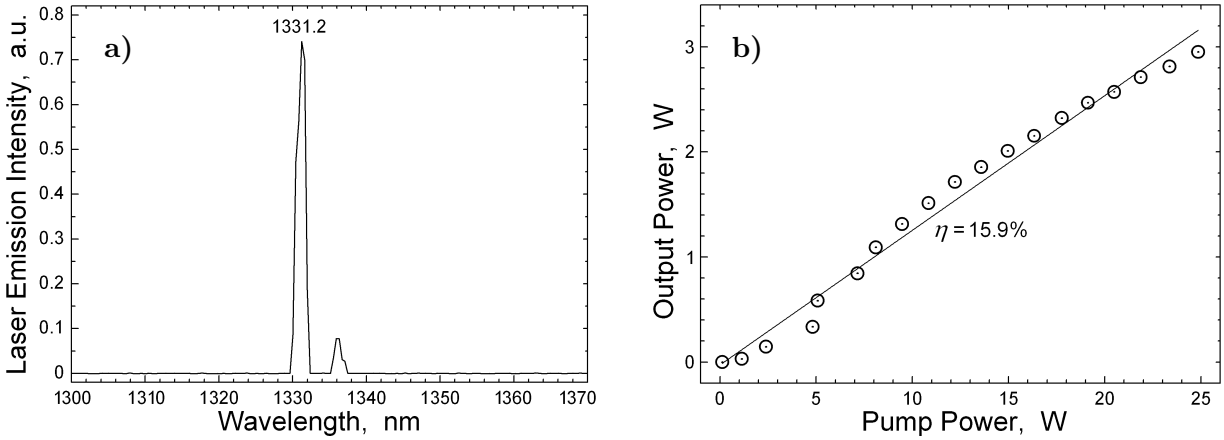

Fig. 3. Diode-pumped Nd:GGG laser at 1331 nm in free running; here, the spectral resolution is 0.1 nm.

When a 0.1 mm thickness BK7 glass plate is inserted to balance the gain and losses in the laser resonator, we experimentally found that the single-wavelength operations at 1323, 1336, 1338, and 1346 nm rather than 1331 nm are achieved by adjusting the inclination angle of the etalon to 4.2°, 3.2°, 1.2°, and 2.0°, respectively. The characteristics of these emission lines and the output powers of the lines are shown in Fig. 4. The maximum powers are 1.94, 1.92, 1.80, and 1.17 W, and the corresponding slope efficiencies are 8.07%, 7.98%, 7.48%, and 4.85%, respectively. Also note that when the etalon is introduced inside the cavity under a single wavelength at 1331 nm, the threshold pump power increases from 1.13 to 1.35 W, and the maximum output power reduces to about 2.46 W; see Fig. 4 b, f. This is mainly due to the

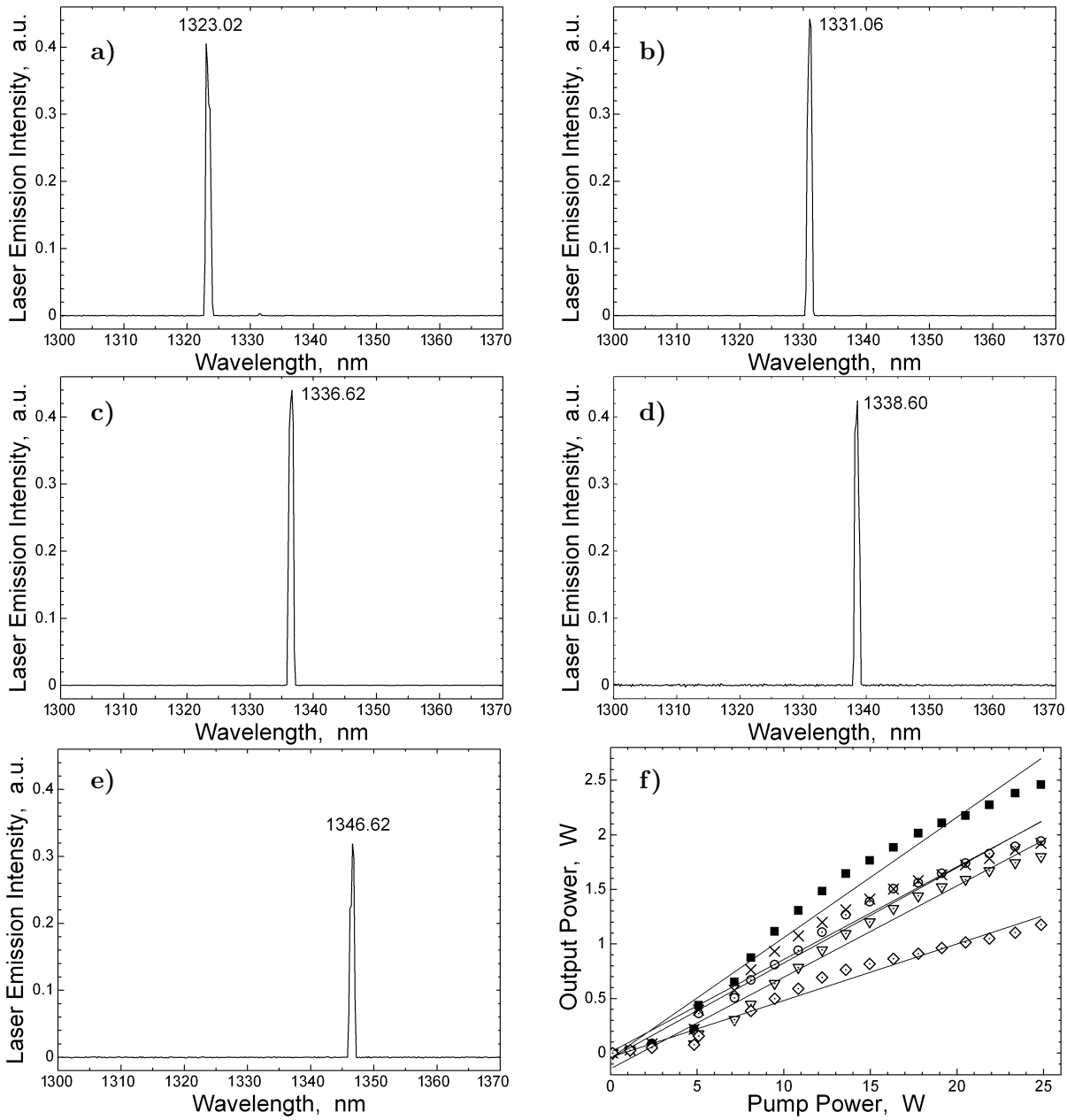

Fig. 4. Etalon-forced diode-pumped Nd:GGG laser at 1323 (a), 1336 (b), 1338 (c), and 1346 nm (d), respectively. Output vs pump power is shown in (f) for 1323 nm $\eta = 8.07\%$ ($\odot$), for 1331 nm $\eta = 10.25\%$ ($\blacksquare$), for 1336 nm $\eta = 7.98\%$ ($\times$), for 1338 nm $\eta = 7.48\%$ ($\triangledown$), and for 1346 nm $\eta = 4.85\%$ ($\lozenge$); lines show the linear fits.

losses caused by the BK7 etalon. To estimate the glass plate insertion losses, we adopted an approximate expression $L = 2\,\theta R d/n\omega$ given in [23], where θ is the incident angle, R is the reflectivity of etalon, d is thickness, n is the refractive index, and ω is the laser beam radius inside the etalon. The insertion losses introduced by the glass etalon can be estimated to be around 0.3% in this experiment.

Moreover, finely adjusting the tilting angle of the etalon to 7.5° for balancing the gain and losses

between these intermanifold lines, we observe that the Nd:GGG laser is operating simultaneously at the three emission wavelengths of 1323.24, 1330.78, and 1336.40 nm; see Fig. 5 where the output power is shown. As a consequence, the maximum output power is 1.66 W and the slope efficiency is 6.6% under a pump power of 24.85 W.

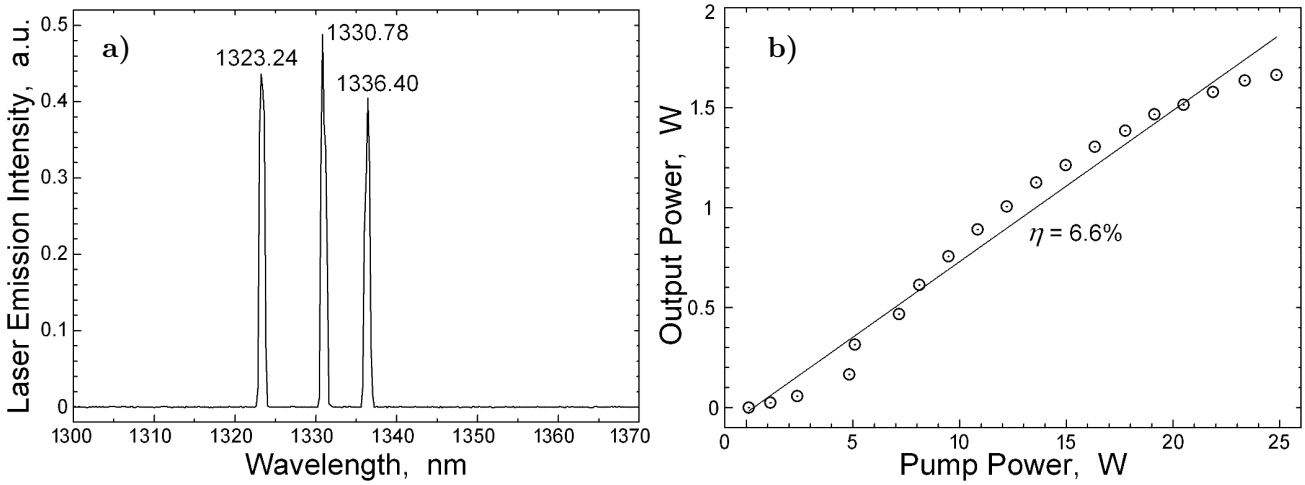

Fig. 5. Etalon-forced diode-pumped Nd:GGG laser operating at 1323.24, 1330.78, and 1336.40 nm.

Now we provide a theoretical analysis of the single- and triple-wavelength lasers operating at 1.3 μm. Tilting the angle of BK7 etalon provides different losses at different lasing wavelengths, exactly as in the case of different single lasing wavelengths. Furthermore, when the gain and losses of different wavelengths are balanced, the simultaneous multiple wavelengths are realized. According to [25], for an etalon with the same reflectivity on the both sides, the transmission of BK7 etalon can be expressed as follows:

$$T = \left[1 + \frac{4r}{(1-r)^2}\sin^2\left(\frac{\delta}{2}\right)\right]^{-1}, \tag{1}$$

with δ being the phase difference caused by light waves passing through BK7, where $\delta = \dfrac{2\pi}{\lambda} 2nd\cos\theta$, nd is the optical thickness of BK7, θ is the angle of the incident light, λ is the laser wavelength, and r is the reflectivity of each reflective surface. When the resonance condition is met, i.e., $2nd\cos\theta = m\lambda$; $m = 1, 2, 3\ldots$, and $T_{\max} = 1$. We use formula (1) to obtain the transmission difference ΔT of two wavelengths (such as 1331 and 1323 nm, and 1331 and 1336 nm) versus the incident angle θ; see Fig. 6. The maximum transmission difference is about 15%, which is experimentally and theoretically confirmed to be enough to suppress the relatively-high-gain 1331 nm lasing. Therefore, the tunable wavelength lasers can be achieved by adjusting the angle of BK7 etalon. In order to achieve simultaneous multiwavelength laser, set the appropriate angle of the BK7 etalon to balance the gain and losses of each emission line. As shown in Fig. 7, when θ is 7.7°, the transmission at 1323, 1331, and 1336 nm is 99.0%, 89.9%, and 97.3%, respectively. The emission cross section of Nd^{3+} at these wavelengths is $3.15 \cdot 10^{-20}$, $3.9 \cdot 10^{-20}$, and $3.5 \cdot 10^{-20}$ cm^2, respectively. The gain and losses could be well balanced to obtain triple-wavelength laser operating at 1323, 1331, and 1336 nm simultaneously; see Fig. 5 a.

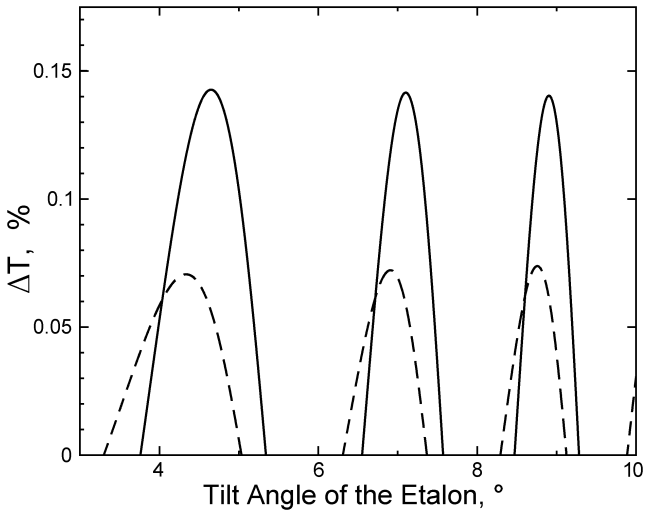

Fig. 6. Transmission difference curves of the 0.1 mm glass etalon between 1331 nm and its two adjacent peaks at 1323 (the solid curve) and 1336 nm (the dashed curve).

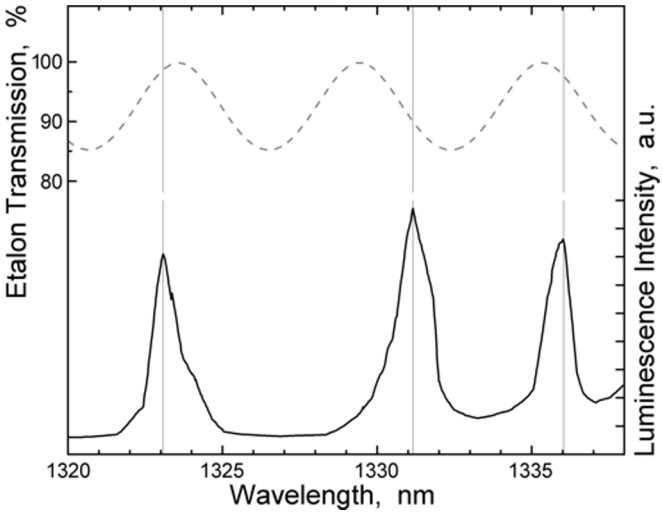

Fig. 7. Glass plate transmission for a tilt angle of 7.5° (the dashed curve) and luminescence spectrum (the solid curve) of Nd:GGG in the range of 1320.0 to 1337.5 nm.

4. Conclusions

We designed and realized a free-running operation at 1331 nm lasing with 880 nm laser-diode pumped Nd:GGG with a maximum output power of 2.95 W and a slope efficiency of 15.9%. Compared with the pumping of 808 nm LD, the output power was greatly improved, which showed that the direct pumping of 880 nm LD is more conductive to high-power laser. When a 0.1 mm thick BK7 etalon was inserted into the laser resonator, tunable lasing wavelengths at 1323, 1331, 1336, 1338, and 1346 nm were achieved. Tilting the angle of BK7 etalon to 7.5°, the gain and losses of the 1323, 1331, and 1336 nm wavelength lasing achieved a good balance, the simultaneous output of these three wavelengths was realized with a maximum output power of 1.66 W. Hope that the study presented has a practical significance for the research on the generation of terahertz waves.

Acknowledgments

The authors thank the financial support provided in part by the Fujian Province Natural Science Foundation under Grant No. 2018J01568, the Scientific Research Scaling Plan of the Xiamen University of Technology under Grant No. XPDKT19005, and the Graduate Science and Technology Innovation Program of the Xiamen University of Technology under Grant No. YKJCX2019060.

References

1. J. P. Boquillon, O. Musset, H. Guillet, et al., "High efficiency flashlamp-pumped lasers at 1.3/spl μ/m with Nd-doped crystals: Scientific and medical applications," in *Technical Digest. Summaries of papers presented at the Conference on Lasers and Electro-Optics. Postconference Edition*, CLEO'99, Conference on Lasers and Electro-Optics (IEEE Cat. No. 99CH37013), 126 (1999); DOI: 10.1109/CLEO.1999.833976

2. J. Fanta, V. Mandys, and L. Horák, *Laser Med. Sci.*, **5**, 317 (1990).
3. H.-Y. Lin, H. Liu, and Y.-P. Wang, *Optik*, **147**, 123 (2017).
4. N. Pavel, V. Lupei, and T. Taira, *Opt. Express*, **13**, 7948 (2005).
5. L. Guo, R. Lan, H. Liu, et al., *Opt. Express*, **18**, 9098 (2010).
6. H. Ogilvy, M. J. Withford, P. Dekker, et al., *Opt. Express*, **11**, 2411 (2003).
7. X. Ding, H. Zhang, and R. Wang, *Opt. Express*, **16**, 11247 (2008).
8. R. Zhou, S. Ruan, C. Du, et al., *Opt. Commun.*, **281**, 3510 (2008).
9. J. Ma, Y. Li, Y. Sun, et al., *Opt. Commun.*, **282**, 958 (2009).
10. Y. Yang, X. Q. Yang, Z. T. Jia, et al., *Laser Phys. Lett.*, **9**, 481 (2012).
11. S. Yiou, F. Balembois, P. Georges, and A. Brun, *Appl. Opt.*, **40**, 3019 (2001).
12. C. Liu, S. Zhao, G. Li, et al., *J. Opt. Soc. Am. B*, **32**, 1001 (2015).
13. Y. F. Lü, X. H. Zhang, J. F. Chen, et al., *Laser Phys. Lett.*, **7**, 699 (2010).
14. M. Boucher, O. Musset, J. P. Boquillon, et al., *Opt. Commun.*, **212**, 139 (2002).
15. H. Li, Z. Wang, F. Zhang, et al., *Opt. Lett.*, **40**, 776 (2015).
16. H. T. Huang, J. L. He, B. T. Zhang, et al., *Opt. Express*, **18**, 3352 (2010).
17. B. Labranche, Q. Wu, and P. Galarneau, *Proc. SPIE*, **2041**, 326 (1998).
18. L. J. Qin, D. Y. Tang, G. Q. Xie, et al., *Laser Phys. Lett.*, **5**, 100 (2008).
19. Z. Jia, X. Tao, C. Dong, et al., *J. Crystal Growth*, **292**, 386 (2006).
20. C. H. Zuo, B. T. Zhang, J. L. He, et al., *Appl. Phys. B*, **95**, 75 (2009).
21. C. H. Zuo, J. L. He, H. T. Huang, et al., *Opt. Laser Techn.*, **41**, 17 (2009).
22. T. Omatsu, M. Okida, A. Lee, et al., *Appl. Phys. B*, **108**, 73 (2012).
23. R. Soulard, B. Xu, J. L. Doualan, et al., *J. Luminescence*, **132**, 2521 (2012).
24. M. Hercher, *Appl. Opt.*, **8**, 1103 (1969).
25. K. Walter, *Solid-State Laser Engineering*, Science Press, Beijing (2002).